Nanorheology of Confined Polymer Melts. 1. Linear Shear Response at Strongly Adsorbing Surfaces

Steve Granick* and Hsuan-Wei Hu

Materials Research Laboratory and Department of Materials Science and Engineering, University of Illinois, Urbana, Illinois 61801

Received December 13, 1993. In Final Form: July 27, 1994[⊗]

The linear-response effective shear moduli of polymer melts confined between strongly adsorbing surfaces (parallel plates of mica) was studied as a function of the excitation frequency. Linear response (achieved with shear amplitudes of ≈2 Å) implies that measurements did not perturb the film structure. The measurements employed a surface forces apparatus modified for dynamic mechanical shear oscillation. The polymers (atactic poly(phenylmethylsiloxane), PPMS, chain length from 31 to 153 skeletal bonds) were selected to be glass-forming with a low glass transition temperature, in order to avoid issues of possible surface-induced crystallization which have been much discussed. Three principal conclusions emerged. First, in a comparison of polymers of different molecular weight, both the shear moduli (measured at fixed film thickness) and the static normal forces (to compress the polymers to this film thickness) scaled approximately with the estimated unperturbed radius of gyration of the chain (R_G). Second, a transition from fluid- to solidlike response occurred when the film thickness was less than 5–6 R_G: the longest relaxation time slowed to the point that the storage shear modulus (G') exceeded the loss shear modulus (G'') over the entire frequency spectrum. This contrasts strongly with the behavior of the bulk samples, for which Rouse dynamics would be expected. Third, the magnitude of G' under conditions of strong confinement was characteristic of rubberlike elasticity, approximately 10^5 N m^{-2} for the range of chain length that was studied. This indicates enhanced entanglement interactions in thin polymer films. Two accompanying papers analyze the nonlinear rheology and the respective influences of surface adsorption and of geometrical confinement.

Introduction

The structure and dynamics of polymer melts near surfaces play an essential role in many diverse physical phenomena, among them polymer–filler interactions in rubbers and composites, polymer adhesives, rheology of colloidal dispersions in paint suspensions, lubrication in magnetic storage devices, and wall-stick conditions in polymer extrusion. In all of these applications, the surface area to liquid volume ratio is large, and the dynamics of polymer molecules near the surface play a central part. On the basis of these facts, a molecular-level understanding of the structure and dynamics of polymer molecules near solid surfaces is of growing interest. Here we expand upon a previous communication.[1]

The distinctive feature of chain molecules at surfaces is that segments of an adsorbed molecule may be located far from the surface yet tethered to it by their skeletal connectivity with other segments that are physically attached to the surface.[2] There is a rapidly growing experimental literature regarding phenomena associated with the structure of polymers which form molecularly-thin films between two solid surfaces. In surface forces experiments with polymer melts, experiments show strong repulsive interactions starting when the film thickness is much larger than the segment size, several times the unperturbed radius of gyration (R_G). This has been reported for poly(dimethylsiloxane),[3,4] polybutadiene (PB),[5] a perfluorinated polyether,[6] and poly(phenylmethylsiloxane) (PPMS).[1] Although the long-range repulsion reported in the first experiments is now recognized to have been not equilibrated, this repulsion is strong, and more recent experiments show it to persist up to the longest experimentally-accessible equilibration time, approximately 24 h per datum.[1] Much theoretical attention has been given to describing the spatial distribution of segments at equilibrium or "restricted" equilibrium, which reflects a competition between the disorderly statistics of a long polymer chain and specific surface–segment interactions.[7,8] It is as if a layer of molecules with thickness approximately 1 radius of gyration were immobilized near each of the solid surfaces.

Thus the structure of polymer fluid at a solid surface has a very different character from that of small molecules. For small molecules the heart of the problem is the local intermolecular order that is analogous to the radial distribution function in the bulk.[2] In general, both the liquid density profile and interaction potential are believed to oscillate with periodicity close to a molecular size, with a decay length of a few molecular dimensions.[2] This layering phenomenon is in principle no different from that in the bulk and is determined primarily by the geometry of the molecules and how they can pack around the constraining boundary. The resulting density oscillations or "structure" is reflected in oscillations in the force needed to compress films to a specified thickness between solid surfaces. For small molecules these structural forces extend up to 5–10 molecular dimensions away from the surface.[2] Attractive interactions between the surface and the liquid molecules lead to a denser-than-bulk packing even of chain segments that are physically located near the surface.[2,9] However, in the case of chain molecules these local packing effects are believed to extend a lesser distance, perhaps only 2–3 segmental dimensions from the surface,[9] owing to the configurational entropy penalty

[⊗] Abstract published in *Advance ACS Abstracts,* September 15, 1994.

(1) Hu, H.-W.; Granick, S. *Science* **1992**, *258*, 1339.

(2) For a review, see: Israelachvili, J. N. *Intermolecular and Surface Forces.*

(3) Horn, R. G.; Israelachvili, J. N. *Macromolecules* **1988**, *21*, 2836.

(4) Horn, R. G.; Hirz, S. J.; Hadziiouannou, G.; Frank, C. W.; Catala, J. M. *J. Chem. Phys.* **1989**, *90*, 6767.

(5) Israelachvili, J. N.; Kott, S. J.; Fetters, L. J. *J. Polym. Sci. Polym. Phys. Ed.* **1989**, *27*, 489.

(6) Montfort, J. P.; Hadziioannou, G. *J. Chem. Phys.* **1988**, *88*, 7187.

(7) de Gennes, P.-G. *C. R. Acad. Sci. Paris* **1987**, *305 II*, 1181.

(8) For a review, see: Ausseré, D. *J. Phys. Fr.* **1989**, *50*, 3021.

(9) Walley, K.; Schweizer, K. S.; Peanasky, J.; Cai, L.; Granick, S. *J. Chem. Phys.* **1994**, *100*, 3361 and references therein.

0743-7463/94/2410-3857$04.50/0

that a chain near the wall must pay to exist in a more highly organized state. A study of poly(dimethylsiloxane) (PDMS)[4] suggests that structural forces exist up to only 1–2 segmental layers.

Apart from questions of static density profiles, what are the dynamics of polymer liquids in intimate contact with a solid boundary? Recent experiments of several kinds, adsorption–desorption dynamics,[10] spreading of droplets,[11] and drainage of polymers in a narrow gap,[12] point to the existence of some kind of general trapped state in this problem—a retarded mobility, commonly termed a "glassy layer", whose origin is poorly understood.[13–15] The prominent part of adsorption in slowing down the center-of-mass motion of an adsorbed chain has been emphasized, based upon computer simulations.[16,17]

In our laboratory, a surface forces apparatus[18] with oscillatory shear attachment[19,20] is used to probe the shear dynamical response of confined liquid molecules. In the experimental setup, liquids are confined between two parallel mica sheets driven by fine motor control down to a film thickness less than 100 Å. The dynamical storage and loss moduli can be measured in a broad range of frequency (0.03–260 Hz) and amplitude (0.5 Å to 1 μm).

Three fundamental questions have been studied: (1) What are the generic dynamics of confined liquids?[19,21] (2) For small molecules, what is the variation in dynamical response due to molecular architecture?[22,23] (3) What is the complexity in dynamics introduced by the long chain connectivity of polymer melts?[1,24]

A few words are appropriate regarding the choice of shear amplitudes of ≈2 Å. The purpose is to achieve a condition of linear response, which implies that measurements did not perturb the film structure; this point is discussed further below. However, the reader may be tempted to question—since 2 Å is actually less than the thickness of the polymer repeat unit—whether a shear amplitude of 2 Å will give a realistic measure of typical molecular motions. In considering this point, one should consider the shear amplitude scaled by the sample thickness (the "strain"): a shear amplitude of 2 Å amounted, in these experiments, to a strain of several percent. In fact, this is in the typical range in everyday viscoelastic studies of molten polymers[34] and is actually larger than required to achieve linear response of crystalline or glassy materials. Accordingly, we emphasize that 2 Å of movement across the thickness of our thin-film samples was typical of the usual conditions in studies of linear response in molten polymer samples even of macroscopic size.

Table 1. Molecular Characteristics of the PPMS Samples

code	M_n[a] (g mol^{-1})	M_w/M_n[b]	n_n[c]	R_G[d] (Å)
polymer A	2240	1.08	31	9
polymer B	4550	1.14	65	13
polymer C	10560	1.16	165	20

[a] Number-average molecular weight. [b] Ratio of weight-average to number-average molecular weight. [c] Number-average number of skeletal bonds. [d] Unperturbed radius of gyration, estimated from the chain length by a rotational isomeric states calculation.[30]

In this study of linear viscoelastic response, we find a more complex response than is typical of small molecules. In an accompanying paper,[25] we show that this correlation breaks up at high strain amplitudes, as reflected in prominent nonlinear viscoelasticity. In another accompanying paper,[25] the linear response between weakly adsorbing surfaces confirms the general patterns described below.

Experimental Section

Polymer Samples. The polymer fluids, atactic methyl-terminated poly(phenylmethylsiloxane) (PPMS),[26,27] were generously donated by S. J. Clarson of the University of Cincinnati. The PPMS is comprised of amorphous and flexible chains that do not crystallize because they are atactic. The bulk glass transition ($T_g \approx -30$ °C)[27] is well below the temperature of these experiments (26 ± 0.5 °C).

The inability to crystallize avoids complications of possible surface-induced crystallization that have been much discussed.[28,29] The low T_g avoids glassy dynamics complications that have been much discussed.[13–15]

Molecular characteristics of the samples studied are given in Table 1. The unperturbed radius of gyration (R_G) was estimated from the chain length by a rotational isomeric states calculation.[30] The persistence length of atactic PPMS in the bulk, estimated from the characteristic ratio, is about 6 skeletal bonds.[30] Although we have no direct measurement of the entanglement length of PPMS (because of a limited amount of sample), from the calculated chain stiffness[30] one expects that the molecular weight between entanglements is $M_e \approx 12\,000$ g mol^{-1},[31] so that chains of the length studied here would be too short to be entangled in the bulk, and Rouse dynamics would be expected.

The polymers wet the mica surfaces with a contact angle of zero. Control experiments, in which PPMS was displaced from mica by water, showed that adsorption was reversible.

We estimate the strength of adsorption to mica as 3–5kT per repeat unit, based on the surface energy of mica cleaved in ambient atmosphere, 200–400 mJ m^{-2}.[2] This estimate is described elsewhere.[9] In fact, the energy to cleave mica in vacuum is considerably higher,[2] so if gases adsorbed onto the cleaved mica surface from the air were to have dissolved into the PPMS liquids during the course of these experiments, one should expect the strength of adsorption to the solid surface to rise. The estimate of 3–5kT per repeat unit is therefore a conservative estimate of the actual adsorption strength.

Experimental Protocol. The surface forces apparatus allows the measurement of static force, versus surface separation, at separations down to molecular dimensions.[18] The experimental protocol used in our laboratory for static surface forces measurements was described in detail previously.[32] Briefly, the mica surfaces were cleaved in a laminar flow hood and were sputtered

(10) Johnson, H. E.; Douglas, J. F.; Granick, S. *Phys. Rev. Lett.* **1993**, *70*, 3267 and references therein.
(11) Silberzan, P.; Léger, L. *Macromolecules* **1992**, *25*, 1267 and references therein.
(12) Chan, D. Y. C.; Horn, R. G. *J. Chem. Phys.* **1985**, *83*, 5311.
(13) de Gennes, P.-G. In *Liquids at Interfaces*; Charvolin, J., Joanny, J. F., Zinn-Justin, J., Eds.; Elsevier: Amsterdam, 1990; Les Houches, Session XLVIII.
(14) Kremer, K. *J. Phys. (Paris)* **1986**, *47*, 1269.
(15) Chakraborty, A.; Shaffer, J. S.; Adriani, P. M. *Macromolecules* **1992**, *24*, 2470.
(16) Thompson, P. A.; Grest, G. S.; Robbins, M. O. *Phys. Rev. Lett.* **1992**, *68*, 3448.
(17) Bitsanis, I. A.; Pan, C. *J. Chem. Phys.* **1993**, *99*, 5520. Gupta, S.; Koopman, D. C.; Westermann-Clark, G. B.; Bitsanis, I. A. Preprint.
(18) Israelachvili, J. N.; Adams, G. E. *J. Chem. Soc., Faraday Trans. 1* **1978**, *74*, 975.
(19) Van Alsten, J.; Granick, S. *Phys. Rev. Lett.* **1988**, *61*, 2570.
(20) Peachey, J.; Van Alsten, J.; Granick, S. *Rev. Sci. Instrum.* **1991**, *62*, 463.
(21) Granick, S. *Science* **1991**, *253*, 1374 and references therein.
(22) Carson, G. A.; Hu, H.-W.; Granick, S. Unpublished experiments.
(23) Reiter, G.; Demirel, A. L.; Granick, S. *Science* **1994**, *263*, 1741. Reiter, G.; Demirel, A. L.; Peanasky, J.; Cai, L. L.; Granick, S. *J. Chem. Phys.* **1994**, *101*, 2606.
(24) Van Alsten, J.; Granick, S. *Macromolecules* **1990**, *23*, 4856.
(25) Granick, S.; Hu, H.-W.; Carson, G. Accompanying paper. Peanasky, J.; Cai, L. L.; Granick, S.; Kessel, C. R. Accompanying paper.
(26) Clarson, S. J.; Dodgson, K.; Semlyen, J. A. *Polymer* **1987**, *28*, 189.
(27) Clarson, S. J.; Semlyen, J. A.; Dodgson, K. *Polymer* **1991**, *32*, 2823.
(28) Schoen, M.; Rhykerd, C. L., Jr.; Diestler, D. J.; Cushman, J. H. *Science* **1989**, *245*, 1223.
(29) Thompson, P. A.; Robbins, M. O. *Science* **1990**, *250*, 792; *Phys. Rev. A* **1990**, *41*, 6830.
(30) Mark, J. E.; Ko, J. H. *J. Polym. Sci. Polym. Phys. Ed.* **1975**, *13*, 2221.
(31) Aharoni, S. M. *Macromolecules* **1983**, *16*, 1722.
(32) Hu, H.-W.; Granick, S. *Macromolecules* **1990**, *23*, 613.

with 600 Å silver film on the backside immediately. A pair of mica surfaces of the same thickness (2–4 μm) was mounted on a silica lens with 1,5-diphenylcarbazide glue. The cleanliness of the mica surfaces was checked by the strong van der Waals attraction in air. The fringe positions in air contact were calibrated.

Due to the limited amount of polymer sample, the polymers were used as received. The polymers were added between the mica surfaces by a pipette that had been flame-sealed at the tip. Phosphorus pentoxide (P_2O_5) was put within the chamber to remove moisture from the system. After at least 2 h of equilibration, the cleanliness of the polymer was checked. Particles or contaminants generally resulted in a shear output signal that was damped at large distances. The experiment was aborted in these rare situations. Provided that the system appeared to be clean, the waveforms of the out-of-contact shear calibration signals were collected at frequencies and amplitudes intended for the experiment.

The surfaces were gradually pushed into contact, and the force–distance profile was measured. At constant film thickness, the frequency was varied to probe the dynamic shear response. This was repeated at several distances of decreasing film thickness. After these measurements were completed, the cleanliness of the system was double-checked to make sure that the data were valid.

After all measurements on the polymer film were completed, distilled water was added to the system to drive the surfaces to strong adhesive contact to the exclusion of polymer. Because gases are adsorbed onto the mica from air, polymer film thicknesses were usually ≈4–6 Å thicker relative to water contact calibration than to air contact calibration.

Dynamic Mechanical Experiments. In oscillatory shear measurements, opposing crossed cylinders are flattened at their tips to produce parallel plate geometry.[19,20] Fluid films, confined in this way, are surrounded by a droplet reservoir, introduced as described above.

Precise measurement and control of the shear strain and forces are accomplished through electromechanical transducers (piezoelectric bimorphs), which permit detailed information about the mechanical responses of the liquid to be acquired with the ease of simple electrical measurements.

The idea of the mechanical model proposed by Peachey[20] is to replace the device with a combination of effective masses, springs, and dashpots, in a manner similar to the modeling of the Birnboim rheometer as reported by Massa and Schrag.[33] The spring constants are determined by calibrations described elsewhere.[20] It is straightforward to write down Newton's equations of motion for the mathematical model. Far from the resonance condition, it is feasible to regard the rheometer as a linear device and to solve these equations to first-order approximation in the angular frequency.

A typical example of comparing the measured signal and calibration is shown in Figure 1. The dynamic moduli are related to the spring constant (k_L) and dashpot coefficient (ωb_L) of the liquid by the geometry factor of the rheometer:

$$G' = (h/A)k_L \quad (1)$$

$$G'' = (h/A)\omega b_L \quad (2)$$

where A is the area of contact, h is the film thickness, and ω is the angular frequency of sinusoidal oscillation. The loss modulus, $G''(\omega)$, is the component of the normalized oscillatory stress that (following Newton's law of viscous flow) was in phase with the rate of deformation. The storage modulus, $G'(\omega)$, is the component of normalized oscillatory stress that (following Hooke's law of elastic deformation) is in phase with the deformation.

The spring constant and dashpot coefficient of the liquid are obtained from the experiments in which a sinusoidal time-varying shear force is applied and the amplitude and phase of response are measured. The calibration and experimental procedure are described elsewhere.[20]

(33) Massa, D. J.; Schrag, J. L. *J. Polym. Sci. A-2* **1972**, *10*, 71.
(34) For a review, see: Ferry, J. D. *Viscoelastic Properties of Polymers*, 3rd ed.; Wiley: New York, 1980.

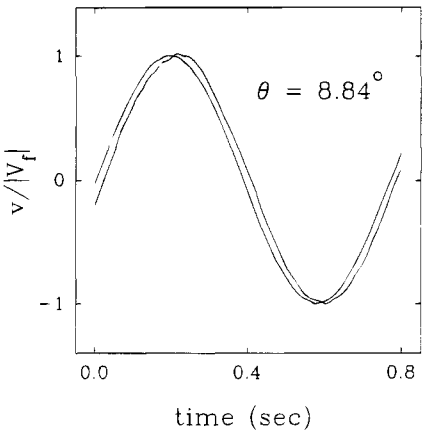

Figure 1. Example of raw data. Shear response and calibration waveforms of polymer B, film thickness 63 Å, plotted versus time. The drive oscillation is 1.3 Hz with amplitude 2 Å. Response lags the calibration by 8.84°. The signals were collected after co-adding 500 cycles of shear oscillation.

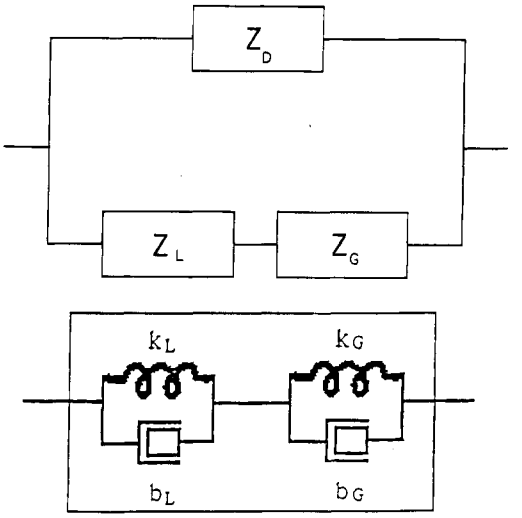

Figure 2. Model used to separate sample response from apparatus compliance. Contributions from the mechanical impedance of the piezoelectric device itself (Z_D), and from a serial contribution of the glue and the sample of interest (Z_G and Z_L, respectively) respond to applied force in parallel. The original spring–dashpot model described in detail in ref 20 (spring constants k, dashpot coefficient ωb) is modified by considering that the measurements probe the serial combination of Voigt elements of the glue (k_G, ωb_G) and the liquid (k_L, ωb_L). Calibrations of k_G and b_G, as a function of frequency, are made with the mica surfaces in adhesive contact in air.

Compliance of the Device. An ideal rheometer should be stiff and have no compliance to the applied forces. As this laboratory has not described previously the correction for the influence of mechanical deformation within the device itself (especially the glue that attached the mica to the rest of the device),[20] we describe this below in detail.

Device compliance was accounted for by a mechanical circuit, shown in Figure 2, in which the calibrated properties of the device and glue were combined with the mechanical response of the sample of interest. Here the mechanical impedance of the piezoelectric device itself (Z_D), and of the serial contribution of the glue and the sample of interest (Z_G and Z_L, respectively), responds to applied forces in parallel. As described in ref 20, the complex impedance of each impedance element can be represented in turn by a parallel ("Voigt") arrangement of elastic and dissipative elements: a spring constant (k) and a dashpot coefficient (b).

The applied force divides into some portion which acts to deflect the piezoelectric device and some portion which acts to deflect the serial combination of glue and sample. Then the measured deflection of the receiver bimorph is equal to the sum of the

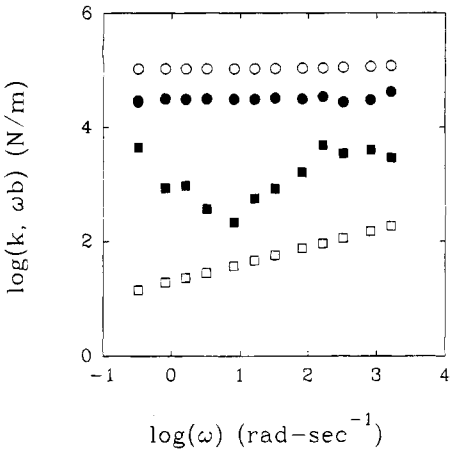

Figure 3. Comparison of the spring constants (k; circles) and dashpot coefficients (ωb; squares) of mica sheets at adhesive contact in air (using DPC glue to mount the mica sheets), and of polymer B of film thickness 34 Å. Measurements, taken at 2 Å shear amplitude, are plotted against angular measurement frequency on log–log scales. Hollow symbols: mica sheets in adhesive contact. Filled symbols: serial ensemble of polymer B plus apparatus compliance ("glue").

deflections within the glue and within the sample of interest. The total complex impedance of this serial combination of sample and glue, $Z = (k + i\omega b)$, is written in terms of the complex impedance of the liquid, $Z_L = (k_L + i\omega b_L)$, and the glue, $Z_G = (k_G + i\omega bG)$:

$$1/Z = 1/Z_L + 1/Z_G \tag{3}$$

The form of this equation becomes obvious in the limit of absolutely-stiff glue; then the equation reduces to $Z = Z_L$. It is straightforward to solve eq 3 mathematically to find the spring constant k_L and dashpot coefficient ωb_L of the liquid in measurable quantities, k, b, k_G, and b_G,

$$k_L + i\omega b_L = (k + i\omega b)\left(\frac{k_G^2 + \omega^2 b_G^2 - kk_G - \omega^2 bb_G}{(k_G - k)^2 + \omega^2(b_G - b)^2} + i\frac{\omega(k_G b - kb_G)}{(k_G - k)^2 + \omega^2(b_G - b)^2}\right) \tag{4}$$

Here we note that the analysis of Peachey[20] is based on comparing the piezoelectric output signal in free oscillation and in the presence of a sample; with respect to this *output* response, the influence of Z_D is already accounted for. However, when one wishes to calculate an *input* force, especially the force that was applied to the sample, the effect of Z_D in partitioning the applied force must be taken explicitly into account.[23]

The complex impedance of the apparatus itself, or "glue" (Z_G), is calibrated by pushing the surfaces into adhesive contact in dry air, without the presence of liquid, in which case $1/Z = 1/Z_G$ in eq 3. The validity of this calibration rests in part on the assumption that the mechanical properties of the devices are the same at high-pressure adhesive contact as at low-pressure experimental conditions (<1 MPa). An additional assumption is that adsorbed gas films do not contribute to this calibration response. To test this latter assumption, control experiments were made, in which a droplet of water was used in place of air in search of a strongly adhesive contact. No resulting stiffening of the measured device compliance was observed. This lends confidence to the supposition that adsorbed gas films did not contribute significantly to the calibration response.

An additional test of this assumption consisted in joining the opposed mica sheets by a cyanoacrylate ("superglue") adhesive. Again, the inferred device compliance was found to be the same as in adhesive contact in dry air. We are indebted to A. Levent Demirel, in this laboratory, for performing this control experiment.

An illustration of k and ωb, of the glue alone and of polymer B in serial combination with glue, is shown in Figure 3. The glue

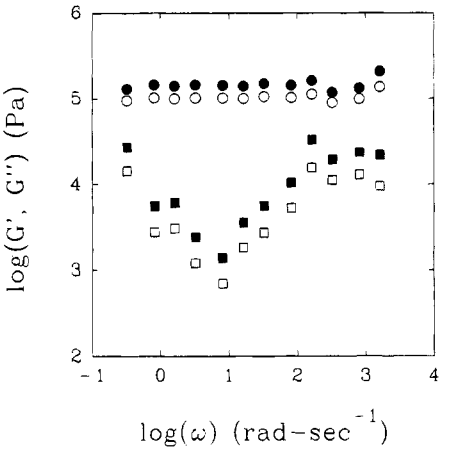

Figure 4. Comparison of linear storage and loss moduli of polymer B, film thickness 34 Å, before (circles) and after (squares) the correction for apparatus compliance. Moduli are plotted against angular frequency on log–log scales. Circles: $G'(\omega)$. Squares: $G''(\omega)$.

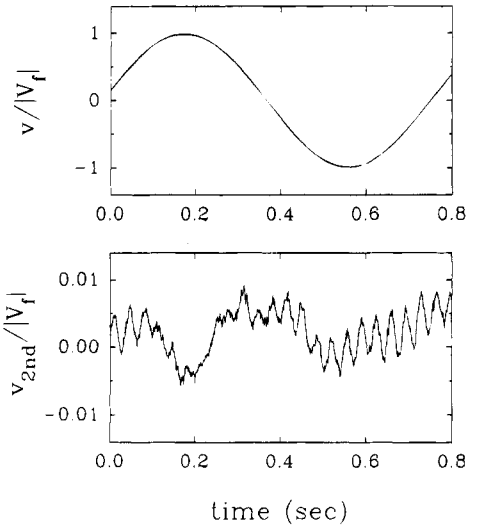

Figure 5. Test for second harmonic response, which would indicate device asymmetry. Top panel: normalized calibration waveform at frequency 1.3 Hz and amplitude 24 Å. Bottom panel: component at frequency 2.6 Hz, normalized by the amplitude of the calibration.

calibration was obtained by mounting the mica sheets onto crossed cylinders of silica using 1,5-diphenylcarbazide (DPC) as glue. The sample was polymer B (described below) of film thickness 34 Å. In Figure 3, one observes that the dashpot coefficient of the glue was small compared to that of the sample and that the spring constant of the glue was larger than that of the sample. Figure 4 illustrates the storage and loss moduli of the serial combination of glue and sample (open symbols) and of the inferred response of the sample itself (filled symbols). The glue correction increases the moduli by a factor 2 or less in this case. The shapes of the moduli–frequency curves remain qualitatively unchanged. The analysis suggests that the correction is needed when the spring constant of the confined liquid is within an order of magnitude of that of the device.

Symmetry of the Rheometer Waveforms. Building piezoelectric devices is delicate work. In the present design, symmetry with respect to the sender and receiver bimorphs is required for reliable operation. If the oscillation is not symmetric in the two shear directions, higher-order even harmonics are generated.

The presence of second-order harmonics (output at twice the input frequency, ω_1) is an undesirable indication of device asymmetry. Figure 5 (top panel) displays a normalized calibration waveform at frequency 1.3 Hz and amplitude 24 Å after co-adding 2000 waveforms. The difference between this wave

form and its first harmonic is shown in Figure 5 (bottom panel). This difference, mostly due to 2ω harmonics, has the amplitude ratio 0.004 and is within the experimental tolerance.

Odd Harmonics in the Output Waveforms. When the sample is excited at high strain and responds in a nonlinear fashion, the response is not sinusoidal at frequency ω_1 anymore but also contains higher odd-order harmonics. It is well established that even-order harmonics are not excited, however, due to symmetry considerations: the shear stress, which must take the same sign as the strain, must be an odd function of the strain.[35] Measurements of nonlinear response, in which odd harmonics appear in the output waveforms, are described in the accompanying paper.

Results

Static Force Measurements. The static force to squeeze a polymer film to a given thickness has recieved much attention.[1-9] In the present measurements, special care was given to reach a steady-state response. The surface force in this type of experiment is measured by moving the base of a spring that supports the lower mica surface inward in a stepwise manner. When the base of the spring is moved, viscoelastic drag prevents the surface supported by the other end of the spring from following it instantaneously. Sufficient time must be allowed after each step to reach kinetic stability. Here kinetic stability means no detectable change in film thickness (<1–2 Å) on the time scale of hours. Under full equilibrium conditions, polymers would have sufficient time to desorb and migrate out of the intersurface region, and the surface force would be zero or attractive.[7,8] In practice, full equilibrium conditions are difficult to meet because of the strong adsorption to the surfaces. The strength of this metastable adsorption can be appreciated by considering the adsorption per segment, approximately $3-5k_BT$[9] (k_B is the Boltzmann constant, and T is the absolute temperature). This must be added up over approximately $N^{1/2}$ adsorbed contacts (where N is the degree of polymerization).

The normal pressures required to squeeze films of polymer B to a specified thickness are shown in Figure 6.[1] The mean normal pressure, $P_\perp$ (normal force normalized by the area of the parallel mica plates), is plotted against film thickness (D). The normal pressure rose monotonically at thickness $D < 60-70$ Å ($5-6R_G$) in approximately an exponential fashion. Because the question of equilibration is an essential point, the equilibration time was varied by a factor of nearly 100 (20 min and 24 h per datum) with no discernible effect. Long-range repulsion in these squeezed polymer films was thus kinetically stable over the long time scales studied.

This decisively corroborates earlier measurements taken with shorter equilibration times.[3-6] It suggests interpretation in terms of the energy to squeeze a fixed adsorbance of tethered polymer.

Normalizing the distance scale by R_G from Table 1 gives the logarithmic force (normalized by area of contact) to compress films of polymer of three different chain lengths shown in Figure 6 (insert). One observes that the force grew monotonically at $D < 5-6R_G$. The relationship was approximately exponential for all three polymer samples.

The orthodox explanation in this area was most clearly enunciated by de Gennes.[7] In this model, polymer segments can be pinned to an adsorbing surface not only directly by adsorption but also indirectly through their connection through the chain to other segments that themselves are adsorbed. A simple estimate shows that

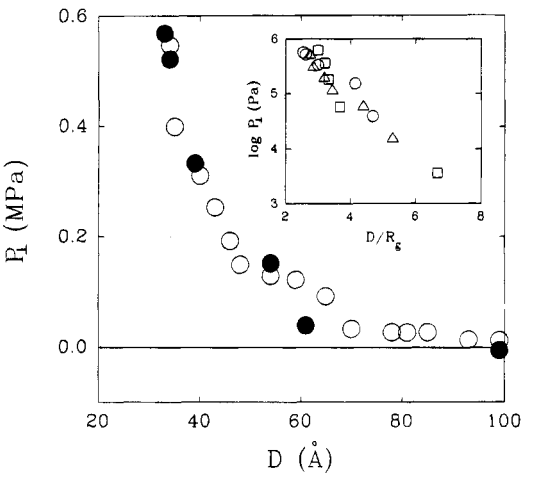

Figure 6. Static pressure in the normal direction required to squeeze a film of polymer B to the specified film thickness. Open circles: equilibration time 20 min per datum. Filled circles: 24 h per datum. Insert: Pressure–distance profiles of polymers A–C. The logarithmic pressure required to squeeze a film to the specified film thickness is plotted against film thickness normalized by the radius of gyration, R_G. The onsets of appreciable surface force and hard wall repulsion are $\approx 4.5R_G$ and $\approx 2.8R_g$, respectively. Squares: polymer A. Circles: polymer B. Triangles: polymer C.

the fraction of segments that are tethered in this fashion decay in a Gaussian fashion with distance normal to the solid surface, with decay length equal to the unperturbed radius of gyration (R_G). Upon confinement, repulsive forces of a Gaussian form, $k_BT \exp[-K(D/R_G)^2]$, emerge which reflect single-chain conformational restriction. In this equation, K indicates a constant. Such a mechanism is qualitatively consistent with the available data (Figure 6). The prefactor, and hence numerical magnitude of the force, is not, however, predicted by the model, as emphasized elsewhere.[36] Moreover, taken at face value, the data seem better described by a simple exponential, not Gaussian, law.

It is interesting to consider another mechanism, proposed by Schweizer,[36] which also appears to lead to monotonically repulsive forces. For dense bulk polymer melts, the intermolecular correlations between a pair of segments on different chains possess a long-range "correlation hole" component due to the combined constraints of chain connectivity and excluded volume.[37,38] From the data in Figure 6 it is difficult to discriminate quantitatively between these (or other) approaches, especially in view of the limited range of R_G. Future experiments are needed to resolve this point.

Linear Viscoelastic Shear Measurements. It is well known that periodic oscillation at radian frequency ω is qualitatively equivalent to probing the dynamic response on the time scale $t \approx 1/\omega$.[34] If the deformations are sufficiently small to give a linear response (stress directly proportional to strain), the measurements are believed to probe the time scales of response that characterize the unperturbed structure of the sample.

Comment regarding the presentation of this data is appropriate. Although the fluids in the experiment were surely inhomogeneous, it is for want of a better way to analyze the data that we have reported it, assuming well-known continuum relations[34] as apparent storage and loss shear moduli, $G'(\omega)$ and $G''(\omega)$. We ignore possible edge

(35) For a review, see: Dealy, J. M. *Melt Rheology and Its Role in Plastics Processing*; Van Nostrand Reinhold: New York, 1990. Matsumoto, T.; Segawa, Y.; Warashina, Y.; Onogi, S. *Trans. Soc. Rheol.* **1973**, *17*, 47.

(36) Hu, H.-W.; Granick, S.; Schweizer, K. S. *J. Noncryst. Solids*, in press.

(37) de Gennes, P.-G. *Scaling Concepts in Polymer Physics*; Cornell University Press: Ithaca, NY, 1979.

(38) Schweizer, K. S.; Curro, J. G. *Chem. Phys.* **1990**, *149*, 105.

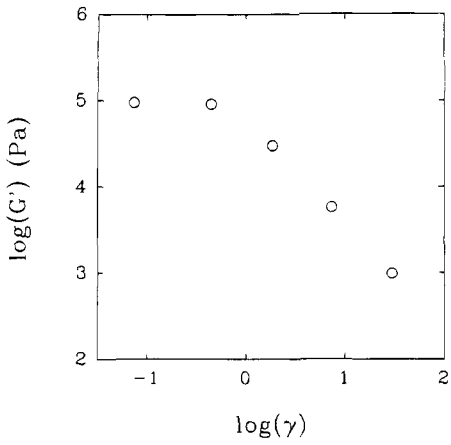

Figure 7. Strain dependence of the storage modulus, for polymer A at film thickness 27 Å. Measurements at 0.26 Hz are plotted versus strain amplitude on log–log scales. The storage modulus is denoted G_1' because, as discussed in the text, it was calculated from the fundamental component of response.

effects and assume that the length scale by which to normalize the shear amplitude is the film thickness. It is true that, on physical grounds, one expects a region of polymer segments near the solid surfaces to have slower mobility, making the rheological film thickness somewhat less than the mica–mica separation.[3-6] However, correction for this effect would not change the relative values of the viscoelastic moduli, nor their orders of magnitude. Because it is not clear how to correct the raw data, we avoided such fine-tuning of the analysis.

Strain Dependence. In order to avoid nonlinear responses, special care was taken to establish the conditions necessary to obtain a linear response. Figure 7 illustrates the strain dependence of the storage modulus, G', for a film of polymer A of thickness 27 Å. Linear behavior held up to strains of ≈30%. In order to ensure linear viscoelastic responses at all the frequencies of measurement, the amplitudes of oscillations applied in the experiments discussed below were maintained at or below 2 Å.

Film Thickness Dependence. The physical picture to imagine is an inhomogeneous system: opposing solid surfaces, each carrying polymer tethered by multiple points of contact, with unattached polymer in between.

We consider first the response at a fixed frequency and variable film thickness. Figure 8 shows the loss and storage moduli for polymer B, measured at 1.3 Hz, and plotted against the film thickness. The data split into two regimes: large thickness, where G' and G'' are comparable in magnitude, and lesser thickness, where G'' passes through a maximum and $G' \gg G''$. This transition is from liquidlike to solidlike behavior.

A logarithmic plot of the moduli confirms this transition, as shown in Figures 9 and 10 for both polymer A and polymer B. This comparison according to chain length shows that these effects set in at larger thickness, the larger the molecular weight. Pronounced dissipation was observed at the relatively large film thicknesses; predominant elasticity was observed at the smaller film thicknesses. At relatively large film thicknesses (but not at smaller ones), dependence on molecular weight was observed, as discussed below.

Effect of Molecular Weight on the Dynamics. We now consider the frequency thicknesses and compare, according to molecular weight.

The limiting response at large film thickness is shown in Figure 11. The storage and loss moduli of polymers A

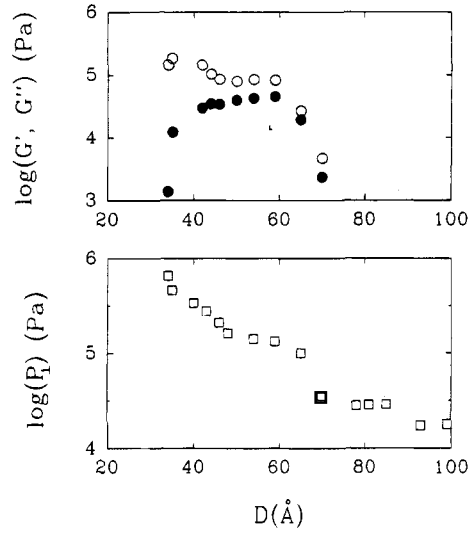

Figure 8. Correlation between shear moduli and static forces in the normal direction. Top panel: storage moduli (open circles) and loss moduli (filled circles) of polymer B, at fixed frequency 1.3 Hz and fixed oscillation amplitude 2 Å, plotted versus film thickness. Bottom panel: corresponding normal pressure, plotted logarithmically versus film thickness.

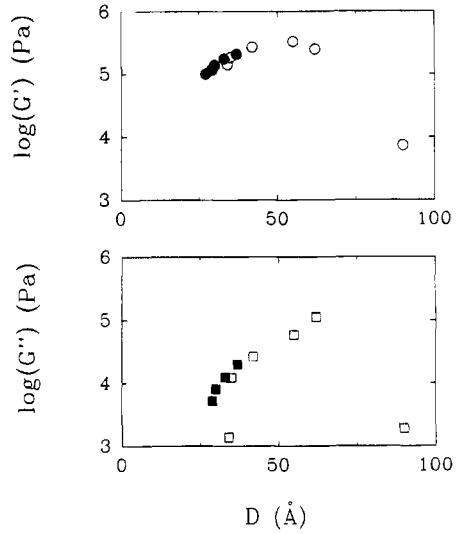

Figure 9. Molecular weight dependence. Storage and loss moduli of polymer A (filled symbols) and polymer B (hollow symbols), at fixed frequency 1.3 Hz and oscillation amplitude 2 Å, plotted versus film thickness on log–log scales. Circles: G'. Squares: G''.

and B are plotted against angular frequency on log–log scales. As expected of bulk viscous flow at low frequency, where G'' must equal $\omega\eta$ (η is the steady-flow viscosity at low shear rate),[34] the $G''(\omega)$ data in Figure 11 have a slope of unity. This result indicates that the inverse frequency of the experiment was larger than the longest relaxation time of the liquid.

The effective viscosity ($G''(\omega)/\omega$) was $\eta_{eff} \approx 100$ Pa s for polymer B and roughly half of this for polymer A (within the scattered data). We distinguish between η_{eff} and a bulk viscosity because the structure of the system was inhomogeneous. These estimates are reasonable for the bulk response of PPMS liquids of this chain length, but we caution that quantitative analysis is difficult because the viscosity of the confined liquid was comparable to that of the bulk liquid. Fluid outside the point of closest approach between the two solid surfaces contributed to these measurements, in contrast to thinner films for which the viscoelastic response of the confined fluids vastly

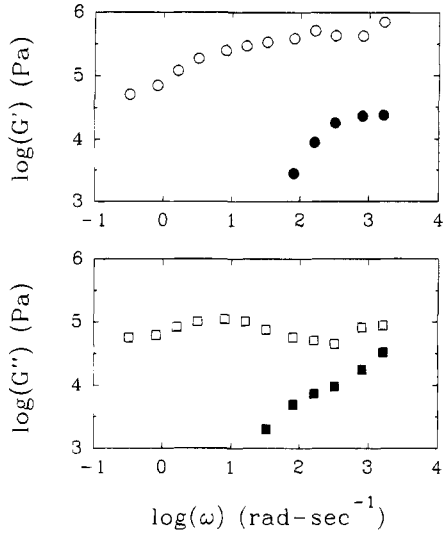

Figure 10. Storage and loss moduli of polymer A (filled symbols) and polymer B (hollow symbols), at fixed film thickness 61 ± 2 Å and oscillation amplitude 2 Å, plotted against angular frequency on log–log scales. Data were taken at 2 Å strain amplitudes. Circles: G'. Squares: G''.

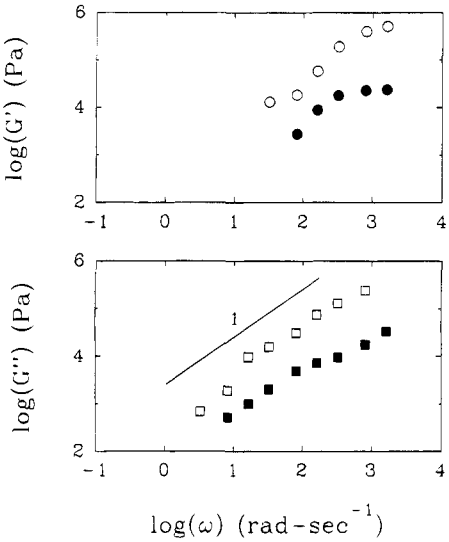

Figure 11. Storage and loss moduli of polymer A (filled symbols) and polymer B (hollow symbols), at fixed normalized film thickness $\approx 7R_G$, plotted versus angular frequency on log–log scales. Circles: G'. Squares: G''. A slope of unity is drawn as a guide to the eye.

exceeded that of the bulk fluid. Nonetheless, in Figure 11, one notes that the larger value of effective viscosity of the sample of larger molecular weight is also reasonable, and qualitatively consistent with the expectation based on the Rouse[34] theory. This was a liquidlike regime.

The physical picture to imagine, as the polymer films were squeezed to a thickness less than $5R_G$, is a progressive interdigitation of the polymer layers that were tethered to the opposing solid surfaces. In this region, extra care had to be taken, after a step increase of the surface force, for equilibration. Each measurement was taken 8 h after a step increase in the surface force. Under these conditions, the film thickness was stable during an experiment and the confined molecules were in a kinetically stable state.

Figure 12 shows the storage and loss shear moduli of polymers A and B, at the thickness of $\approx 4R_G$, plotted against angular frequency on log–log scales. This catches some important features of a transition regime. The storage and loss moduli were both higher than those at

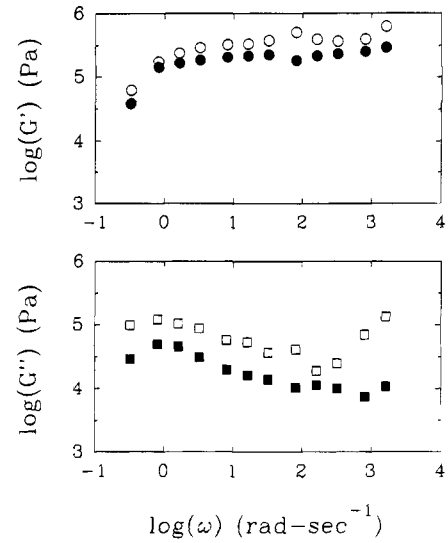

Figure 12. Storage and loss moduli of polymer A (filled symbols) and polymer B (hollow symbols), at fixed normalized film thickness $\approx 4R_G$, plotted versus angular frequency on log–log scales. Circles: G'. Squares: G''.

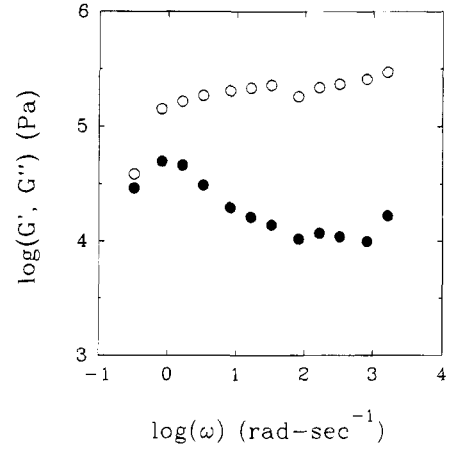

Figure 13. Storage moduli (open circles) and loss moduli (closed circles) of polymer A, at fixed film thickness 37 Å, plotted versus angular frequency on log–log scales. Data were taken at 2 Å strain amplitude.

the same frequency in the liquidlike regime. The storage modulus gradually increased with frequency from 10^5 to 10^6 Pa. The loss modulus crossed the storage modulus at $\omega \approx 1$ rad/s; this suggests a possible terminal relaxation time of $\approx 6\ s^{-1}$. The loss modulus had a shallow minimum at $\omega \approx 330$ rad/s. These dynamic moduli are similar to those of entangled polymer melts in the plateau and the onset of the terminal zones.

Generally speaking, there was an emergence of some kind of restraints which impeded long-time conformational motions; the terminal zone shifted progressively to lower frequencies, and the plateau zone became longer and flatter with increasing confinement.

This splitting of frequency scales is illustrated in Figure 13—just at the point of onset of static forces in the normal direction. In Figure 13, $G'(\omega)$ and $G''(\omega)$ of a film of polymer A 37 ± 1 Å thick ($4.8R_G$) are plotted against radian frequency, ω, on logarithmic axes. The data split into two regimes: low frequencies, where $G'(\omega)$ and $G''(\omega)$ are comparable in magnitude, and higher frequencies, where $G'(\omega)$ exceeds $G''(\omega)$. The frequency at the split defines a relaxation time of the system (in this case ≈ 0.1 Hz). This slow relaxation time can be tentatively identified with the kinetics of attachment and reattachment of the

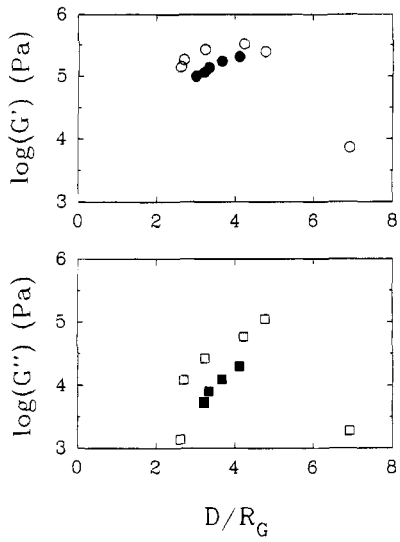

Figure 14. Logarithmic storage moduli (circles) and loss moduli (squares) of polymer A (filled symbols) and polymer B (hollow symbols), at fixed excitation frequency 1.3 Hz, plotted against film thickness normalized by R_G.

adsorbed structures. Qualitatively, the behavior in Figure 13 resembles the conventional viscoelastic behavior of high molecular weight polymer fluids at the transition between terminal and plateau zones.[34]

Finally, the approximate scaling of these effects with the radius of gyration (R_G) of the molecule is shown in Figure 14. The logarithmic storage and loss moduli of polymers A and B are plotted against film thickness normalized by R_G, for data taken at frequency 1.3 Hz. The plateau of the storage modulus at small film thickness, accompanied by a decrease of the loss modulus, is illustrated conclusively. Over the limited range of R_G studied, it is striking how the dynamics scaled qualitatively with this characteristic length of the molecules.

Within the experimental uncertainty, these effects did not depend upon the molecular weight, but this observation must be treated with catuion since the molecular weight was varied over a rather narrow range.

Kramers–Kronig Relations. The relations between the real and imaginary parts of the response to a sinusoidal excitation, known as the Kramers–Kronig relations,[47] allow one to calculate one dynamic mechanical modulus from the other. One approximation of this calculation yields[47]

$$G'(\omega_2) = G'(\omega_1) + \frac{2}{\pi}\int_{\ln \omega_1}^{\ln \omega_2} G''(\omega)\, \mathrm{d} \ln(\omega) \qquad (5)$$

This equation can be used as a quantitative check of the measured moduli. Figure 16 shows the storage modulus of polymer B, at film thickness 55 Å, calculated from the loss modulus through eq 5. The quantitative overlap of the measured and calculated storage moduli shows the consistency of the rheological measurements.

Relaxation Modulus. The linear constitutive equation in simple shear is based on the principle that the effects of sequential effects of shear are additive. Schwarzl proposed an approximate equation to calculate the relaxation modulus $G(t)$ from the storage and loss moduli in linear viscoelasticity:[39]

$$G(t)|_{t=1/\omega} = G'(\omega) - 0.566G''\left(\frac{\omega}{2}\right) + 0.203G''(\omega) \qquad (6)$$

(39) Schwarzl, F. R. *Pure Appl. Chem.* **1970**, *23*, 219.

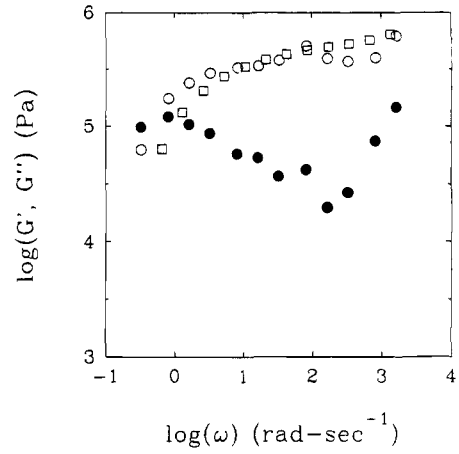

Figure 15. Kramers–Kronig relations used to calculate the G' (squares) from the measured G'' (filled circles). The data refer to polymer B at film thickness 55 Å. The calculated G' agrees quantitatively with the measured G' (hollow circles), illustrating the consistency of the rheological measurements.

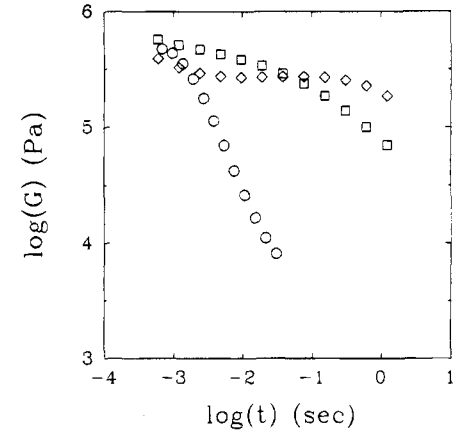

Figure 16. Shear relaxation moduli of polymer B, calculated from dynamic mechanical measurements, plotted versus elapsed time on log–log scales. Thickness is 90 Å (circles), 62 Å (squares), and 42 Å (diamonds).

Figure 15 illustrates this linear relaxation modulus, plotted versus time in the liquidlike (90 Å), transition (62 Å), and plateau regimes (42 Å). The three curves converge at short time scales (10^{-3} s). However, the long-range and long-time ($>10^{-3}$ s) molecular relaxations were gradually frozen by confinement.

Discussion

The experimental evidence presented above suggests that the long-time dynamics of the flexible polymer chain molecules near the adsorbing solid surfaces were frustrated by surface interactions. The static surface forces and the regimes of dynamic response scaled approximately with the radius of gyration. In response to step increases of the normal force which tended to compress the polymer films, some polymer molecules drained out of the gap and others remained within it. The remaining molecules were presumably statistically deformed. It is the dynamical structure of the deformed chains that was probed by the shear measurements.

The polymeric character of the liquid medium thus introduces a sharp distinction between the segmental scale and molecular scale aspects of the problem. On the segmental scale, computer simulation[17,40,41] shows that

(40) Kumar, S. K.; Vacatello, M.; Yoon, D. Y. *J. Chem. Phys.* **1988**, *89*, 5206.

the local density and orientation of segments are somewhat perturbed by the solid surface but that this perturbation is shielded out 2–3 segmental layers from the surface. Beyond this point the segmental density is essentially the bulk value and is independent of molecular weight. This is closely related to the extremely low compressibility of polymer melts, which suppresses any correlation between density fluctuations over distances considerably larger than the segment size. On the molecular scale, however, chain conformations are perturbed by the surface. For linear polymers, this perturbation is believed to be screened out at distances roughly 2 radii of gyration from the surface.[7]

A similar distinction between short-time segmental motions and long-time molecular motions may be useful in analyzing the dynamic aspects of the problem. Surfaces, however, often impose their own time scales, which might obscure this distinction. It is quite possible that short-time segmental dynamics are slowed down drastically in the immediate vicinity of the surface. Such a slowing down of the segmental dynamics (a kind of vitrification of the train segments)[42] will alter the long-time global dynamics of an adsorbed chain molecule. If the segment–surface interaction is strong, there should occur a tethered layer of thickness comparable to the unperturbed radius of gyration. One possible long-time molecular motion is the displacement of the adsorbed chains by the bulk chains; however, the energy barrier for displacement is large, and this rate should be very slow. A second possible long-time molecular motion is the creeping of polymers on the surface proposed by de Gennes.[13] The adsorbed polymers remain tethered to the surface throughout this creeping process.

The emergence of static surface forces and rubberlike dynamics occurred at $\approx 4-5R_G$. This presumably reflects the overlap of two perturbed layers, each of thickness $2R_G$. For the lower molecular weight studied, for which Rouse dynamics are expected in the bulk, the dynamics for $D < 4.5R_G$ would also be typical of a cross-linked or highly entangled rubber in the bulk.[34] The large strain (≈ 0.1) at the onset of a nonlinear response (significantly larger than for a crystal) would also be typical of those systems. Pursuing the analogy, an estimate of the density of effective network strands follows in which the classical equation of rubberlike or entanglement elasticity, $G'(\omega) = (\varrho/M_e)(k_BT)$ is used (ϱ is the density, and M_e is the molecular weight between effective cross-links). The result is that $M_e \approx 6000$ g mol^{-1}. This value is less than the estimated $M_e \approx 12\,000$ g mol^{-1} in the bulk; the comparison must, however, be treated with caution in view of the uncertainty in estimating M_e in the bulk. The main point is that M_e in the thin film obviously is larger than the actual size of the molecules.

Another suggestive calculation involves comparing the bulk longitudinal modulus, M, from force–distance data of the kind shown in Figure 6. Details of this calculation, used to estimate Poisson's ratio (μ) by using standard rheological relations for a continuum system,[34] were described elsewhere previously.[1] Poisson's ratio indicates how much a material contracts when it is extended. When M greatly exceeds the shear modulus, it follows that $\mu = {}^1/_2$ and that no change in volume accompanies the deformation of a material.[34] The calculations show a monotonic rise from $\mu = 0$ ($P_\perp = 0$) to the limiting value expected of a rubber, $\mu \approx {}^1/_2$ (the thinnest films). This we believe to reflect progressive drainage of unattached chains out of the tethered structures. Quantitative calculations of M are shown in ref 1.

What of the dependence on chain length? As we have seen, at $D < 4R_G$, $G'(\omega)$ reached a limiting value that was approximately the same for both samples, $\approx 10^5$ N m^{-2} for both polymers studied. The generality of the phenomenon of frequency-independent elasticity, with rubberlike magnitude, is thus clear. However, we defer detailed quantitative comparison for future study because of the limited range of molecular weight.

These are the central experimental results. Let us now restate the problem to be explained. The high resistance which confined polymer melts present to compression has been discussed previously,[4-9] but strong shear elastic forces are a qualitatively new phenomenon.

Should one suppose that polymer molecules in this narrow gap actually bridged the two solid surfaces, becoming physically attached to both at once? This would produce elasticity in a fashion analogous to the effect of cross-links in a bulk rubber.[43] Simple calculations suggest, however, that the density of bridging would not be sufficiently high to explain the observed magnitudes of elasticity.

What we believe to be a more likely mechanism comes from an analogy with bulk polymers. Uncross-linked, linear polymers of sufficiently high molecular weight also characteristically exhibit a zone on the frequency scale of relatively slow relaxation, where the magnitude of the elasticity is similar to the levels of G' measured here.[34] The phenomenon is believed to reflect caging effects, traditionally referred to as entanglements; polymer chains, as they diffuse, can slide by one another but cannot cut across one another, and chain motions become highly correlated.[44] Similarly, in the system studied here, chains tethered to one surface may be blocked in their motion, over the experimental frequency range, because they cannot cut across other polymer chains that are tethered to the opposing surface. A related suggestion of increased entanglement in a thin film has been made by others.[4] We suggest tentatively that the elastic effects observed here can usefully be viewed as entanglement phenomena—although the chains are too short to be entangled in the bulk.

The motions and relaxations indicated here are thus qualitatively different from those that would characterize the bulk polymer. The frequency-dependent shear forces show the emergence, in these thin films, of a strong elastic component that appeared to reach a limiting value typical of entangled or cross-linked chains in the bulk. The view that entanglement interactions are enhanced in a restricted geometry finds theoretical support.[45,46]

Conclusions

These experiments show a remarkable transition with diminishing thickness. At the onset of repulsive surface forces, the polymer experienced a spectacular liquidlike to rubberlike transition, in which the viscoelastic behavior crossed continuously from that typical of a bulk liquid to that reminiscent of a rubber. The polymer molecules appeared to be correlated to the surfaces over the experimental time scales and to behave as if they were "entangled". The physical picture we suggest is that the changes in viscoelastic response, with diminishing film thickness, reflect progressive drainage of unattached

(41) Bitsanis, I.; Hadziiouannou, G. *J. Chem. Phys.* **1990**, *92*, 3827.
(42) Johnson, H. E.; Granick, S. *Science* **1992**, *255*, 966.
(43) Klein, J.; Luckham, P. F. *Nature* **1984**, *308*, 836.
(44) For a review, see: Doi, M.; Edwards, S. F. *The Theory of Polymer Dynamics*; Oxford: New York, 1986.
(45) Douglas, J. F.; Hubbard, J. B. *Macromolecules* **1991**, *24*, 3163.
(46) Schweizer, K. S. Private communication.
(47) Tschoegl, N. W. *The Phenomenological Theory of Linear Viscoelasticity*; Springer-Verlag: New York, 1989.

chains out of tethered adsorbed structures. The thickness dependence of the dynamic structure may be understood by analogy with the buildup of a polymer network as entanglements are introduced.

Control experiments[25] indicate a similar slowing down of viscoelastic response for these same polymers between weakly-adsorbing surfaces—but at single smaller film thickness, independent of molecular weight, a thickness comparable to the thickness of the PPMS repeat unit. The conclusion as to enhanced entanglement interactions in sufficiently-thin polymer films thus appears to be general—but, in the case of strong adsorption, to develop at a larger film thickness, which increases in proportion to the radius of gyration.

These observations have evident bearing on understanding a variety of physical situations where conforming surfaces separated by molten polymers come into close contact—especially adhesion, spreading, static friction, and lubrication.

Acknowledgment. We are indebted to A. Dhinojwala, J. F. Douglas, J. D. Ferry, G. Reiter, and K. Schweizer for comments and discussions and to S. J. Clarson for donating the PPMS samples used in this study. We thank the Exxon Corp. for generous assistance. S.G. acknowledges support from Grant NSF-MSS-92-02143. We acknowledge support of the National Science Foundation through the Materials Research Laboratory at the University of Illinois, Grant NSF-DMR-89-20538.